# Performance Comparison of Single Sideband Direct-Detection Nyquist-Subcarrier Modulation and OFDM

M. Sezer Erkılınç, *Student Member, IEEE,* Stephan Pachnicke, *Senior Member, IEEE,* Helmut Griesser, *Member, IEEE,* Benn C. Thomsen, *Member, IEEE,* Polina Bayvel, *Fellow, IEEE,* and Robert I. Killey, *Member, IEEE*

***Abstract*—Direct detection transceivers offer advantages, including lower cost and complexity, in short- and medium-haul links. We carried out studies seeking to identify the signal formats which offer the highest information spectral densities and maximum transmission distances for direct detection links. The performance of two spectrally-efficient direct detection optical signal formats, single-sideband (SSB) Nyquist pulse-shaped subcarrier modulation (SCM) and SSB orthogonal frequency division multiplexing (OFDM), are compared by means of simulations. The comparison is performed with wavelength division multiplexing (WDM) net information spectral densities of up to 2.0 b/s/Hz by varying the signal bandwidth, modulation cardinality and WDM channel spacing. The signal formats' tolerance to signal-signal beating interference, resulting from square-law detection, is investigated, and the Nyquist-SCM format is found to suffer lower penalties from this nonlinearity at high information spectral densities. In 7×28 Gb/s WDM transmission at 2.0 b/s/Hz (with electronic pre-distortion and EDFA-only amplification), Nyquist-SCM signals can be transmitted over distances of up to 720 km of standard SMF in comparison to a maximum of 320 km with the OFDM signal.**

***Index Terms*—Optical communication, direct detection, wavelength division multiplexing, Nyquist pulse shaping, subcarrier modulation, orthogonal frequency division multiplexing, signal-signal beating interference, electronic pre-distortion, digital signal processing.**

## I. Introduction

THE demand for high bit-rate transmission using cost-effective solutions is continuously increasing, especially in short and medium reach optical links. In order to meet this demand, multilevel modulation techniques achieving spectrally-efficient transmission are attractive and have started to be utilized in the last decade [1], [2]. The highest information spectral densities (ISDs) have been achieved using polarization multiplexing and coherent detection, enabling full recovery of the optical field, and such systems have become the standard in long and ultra-long transmission links. However, due to their potentially lower complexity and cost, single polarization and direct-detection transceivers may be an attractive solution for shorter distances, such as in short reach optical links, *e.g.*, data centers and interconnect applications, typically up to 10 km, and medium reach optical links, *e.g.*, access and wireless back-haul links as well as metro and regional distances, typically up to 800 km. The cost could be significantly reduced due to the lower number of optical components required, relaxation of the laser linewidth requirements, and the lower complexity of digital signal processing (DSP) at the receiver. A key question then is, what signal formats offer the highest information spectral densities and maximum transmission distances in direct detection links.

A variety of formats have been proposed to achieve high ISD, including pulse amplitude modulation (PAM), optical duobinary (ODB), subcarrier modulation (SCM) (*e.g.*, Nyquist-subcarrier modulation (Nyquist-SCM) and orthogonal frequency division multiplexing (OFDM)) and carrierless amplitude/phase modulation (CAP). PAM is the simplest format but suffers from low receiver sensitivity [3]. ODB transmission has been demonstrated at an ISD of 0.8 b/s/Hz [4] and 1 b/s/Hz [5], but it is fundamentally limited to 1 b/s/Hz. Hence, we focus on single sideband (SSB) subcarrier modulation formats (Nyquist-SCM and OFDM) with quadrature amplitude modulation (QAM) of the RF-subcarrier(s), which are detected by beating with the optical carrier. They enable ISDs greater than 1 b/s/Hz with a good optical-to-signal noise ratio performance. Unfortunately, the receiver sensitivity performance of direct detection SCM formats degrades due to the nonlinear square-law detection, resulting in signal-signal beating interference (SSBI), sometimes referred to as intermodulation distortion.

In this paper, we investigate the transmission performance of SSB Nyquist pulse-shaped SCM and SSB OFDM using direct detection in the presence of SSBI. Their tolerance to SSBI is directly compared by varying the spectral guard band between the optical carrier and sideband in both single channel and wavelength division multiplexing (WDM) system architecture. We consider the use of electronic pre-distortion (EPD), sometimes referred to as electronic dispersion pre-compensation to mitigate the dispersion accumulated along the fibre link for both formats. In the case of OFDM, bit loading is applied to minimize the distortion due to the signal-signal beating interference. Their performance in back-to-back operation, and in transmission over standard single mode fibre (SMF) links (both single channel and WDM system) is assessed by simulations. The comparison is performed at a symbol rate of 7 GBaud with QAM modulation to achieve per-channel bit rates of up to 28 Gb/s and WDM net ISDs of up to 2.0 b/s/Hz assuming the use of hard-decision forward error correction (HD-FEC).

Manuscript received November 28, 2014; revised January 17, 2015. This work was supported by the EU ERA-NET+ project PIANO+ IMPACT and EPSRC UNLOC EP/J017582/1.

M. Sezer Erkılınç, Benn C. Thomsen, Polina Bayvel and Robert I. Killey are with the Optical Networks Group, Department of Electronic and Electrical Engineering at University College London, London WC1E 7JE, U.K. (e-mail: m.erkilinc@ee.ucl.ac.uk; b.thomsen@ucl.ac.uk; p.bayvel@ucl.ac.uk; r.killey@ucl.ac.uk).

S. Pachnicke is at the ADVA Optical Networking SE, Maerzenquelle 1-3, 98617 Meiningen, Germany. (spachnicke@advaoptical.com).

H. Griesser is at the ADVA Optical Networking SE, Fraunhoferstr. 9a, 82152 Martinsried, Germany. (hgriesser@advaoptical.com).

Color versions of one or more of these figures in this paper are available online at http://www.ieeexplore.ieee.org.

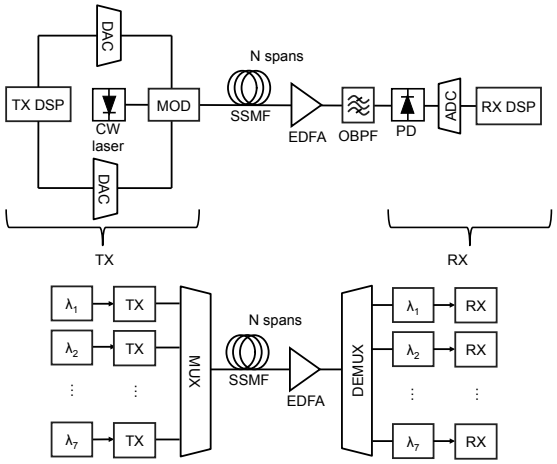


Fig. 1: System architecture for single channel (top) and WDM system (bottom).

## II. Description of Nyquist-SCM and OFDM Techniques

The direct-detected system architecture considered in this paper is shown in Fig. 1. In the direct-detection subcarrier modulation technique, a single or multiple subcarrier(s), also referred to as RF-subcarrier(s), is/are used to transmit data over a fibre link. High-order modulation is achieved by applying QAM to the subcarrier(s) and using linear optical field modulation. At the receiver, the channel of interest is optically demultiplexed by an optical band-pass filter (OBPF) and optical-to-electrical conversion is achieved by a single-ended photodiode, beating between the optical carrier and the sideband during the square-law photodetection. Then, the electrical signal is digitized using a single ADC, as depicted in Fig. 1.

However, the photodetection process generates unwanted additional components, referred to as signal-signal beating products, which interfere with the desired signal, referred to as carrier-signal beating products. This effect is termed signal-signal beating interference (SSBI). One approach to reduce the associated performance degradation is the use of SSBI estimation/cancellation. There are some proposed estimation/cancellation techniques to reduce this interference. However, they result in degradation in receiver sensitivity due to high carrier-to-signal power ratio (CSPR) [6], [7], increased DSP complexity [8], [9], optical complexity or overheads [10], [11]. An alternative approach is to use a spectral guard band between the sideband and the optical carrier with bandwidth, $B_g$ (see Fig. 2). Since the signal-signal beating products bandwidth is equal to the signal bandwidth ($B_s$), the guard band bandwidth must be set such that $B_g \geq B_s$ to avoid any spectral overlap between the carrier-signal and signal-signal beating products. However, this results in a reduction of the ISD by a factor of two and inefficient use of the available bandwidth of RF components used in the system [12]. Alternatively, the bandwidth of the guard band may be set to a lower value, *i.e.,* $B_g < B_s$, to achieve the desired ISD/OSNR penalty trade-off depending on the overlap between the sideband and signal-signal beating products [13]. In the following, to quantify the amount of overlap between the sideband and signal-signal beating products, we use the overlapping ratio parameter, defined as the ratio of the overlapping bandwidth ($B_{ov}$) and $B_s$, as depicted in Fig. 2(b).

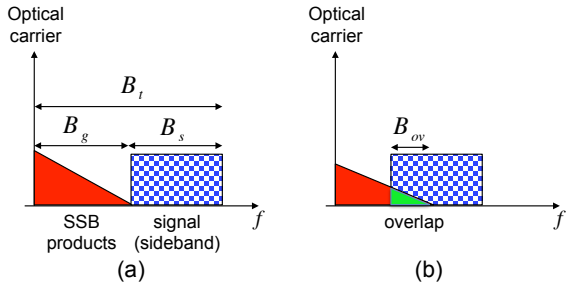


Fig. 2: Spectrum of detected SCM signals (a) non-overlapping and (b) overlapping case. Total bandwidth ($B_t$) is equal to $2B_s - B_{ov}$ where $B_s$ is the signal bandwidth, and $B_{ov}$ is the overlapping bandwidth between the signal and signal-signal beating products. $B_g$ is the spectral guard band between the optical carrier and sideband.

In this paper, we considered two types of spectrally-efficient direct-detection SCM formats: SSB OFDM, and SSB single subcarrier modulation with Nyquist pulse shaping. OFDM is widely used in digital communication systems to achieve high ISD [14]. It is a multi-subcarrier modulation technique in which a data stream is encoded onto multiple densely-spaced orthogonal subcarriers in the frequency domain using the inverse discrete Fourier transform. Although it allows increased ISD with a simple receiver structure, the receiver sensitivity is affected by the high peak-to-average power ratio (PAPR) of the signal, caused by high peaks in signal waveform. They occur due to the constructive addition of the relative phases of the subcarriers [15]. High PAPR results in increased nonlinear distortion, and also increases the required dynamic range of the DACs/ADCs used in the transceiver, causing increased converter quantization noise. The alternative SCM format we considered, single subcarrier modulation, in which a QAM signal is electrically modulated onto a single subcarrier, has potentially lower PAPR compared to OFDM since it utilizes only one subcarrier and avoids the problem of constructive addition of multiple subcarriers. The subcarrier frequency ($f_{sc}$) and roll-off factor of the pulse shaping filter ($\alpha$) are selected according to the required optical ISD and receiver sensitivity requirements. To maximize the ISD, the RF-subcarrier frequency should be close to half of the symbol rate, and the pulse shaping filter should have a roll-off factor close to zero. Single-cycle SCM quaternary phase-shift keying (QPSK) and 16-QAM in which $f_{sc}$ was set equal to the symbol rate ($f_s$), were demonstrated in [16]. In addition to single-cycle, half-cycle ($f_{sc} = f_s/2$) Nyquist-SCM 16-QAM was also demonstrated back-to-back and in transmission over 4 km of standard SMF in [17] to achieve ISD approaching $\log_2(M)/2$. The very close spacing between the optical carrier and subcarrier is enabled by using Nyquist pulse shaping filters with root raised cosine (RRC) transfer function and $\alpha$ of $\leq 0.4$ [18]. For both the OFDM and Nyquist-SCM signal formats considered in this study, the ISDs are increased by digitally suppressing one of the sidebands, referred to as single sideband signalling, to achieve ISD approaching $\log_2(M)$. The trade-off between $\alpha$ and $f_{sc}$ for SSB single SCM was

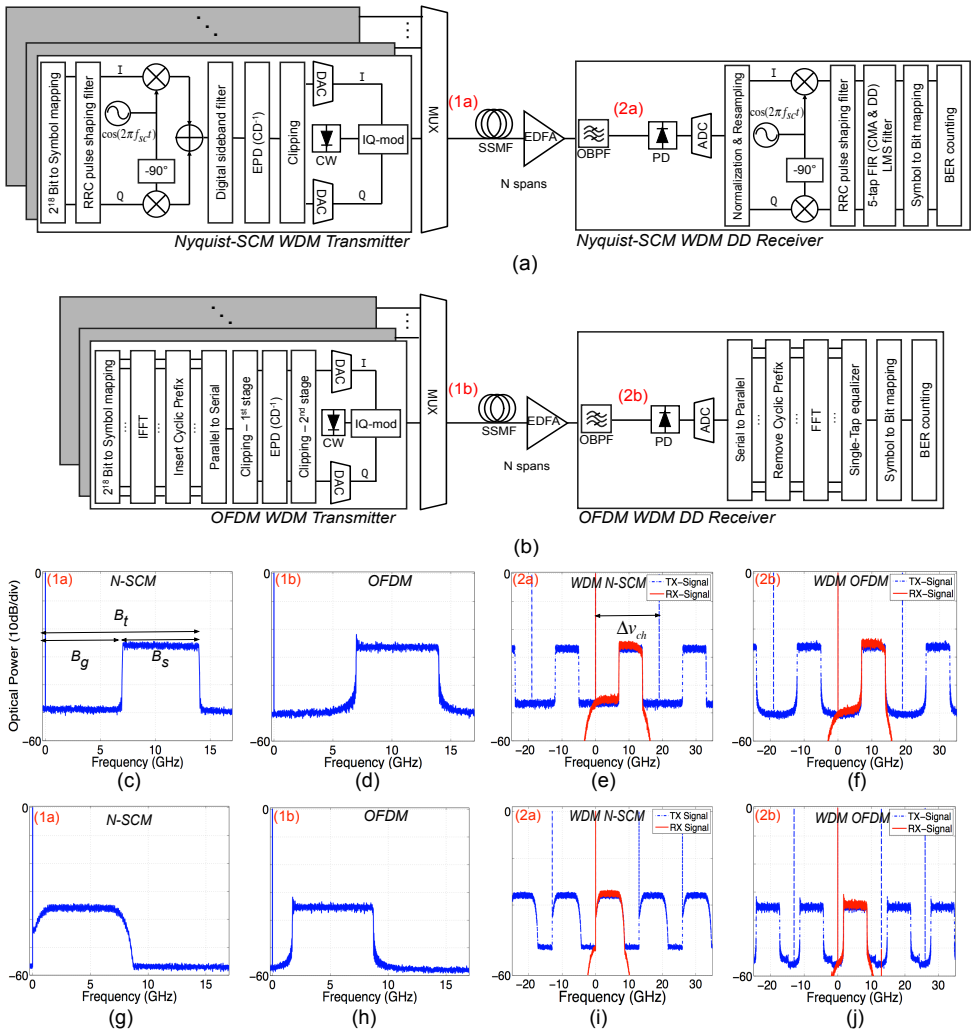


Fig. 3: (a) Nyquist-SCM and (b) OFDM system diagram. Single channel optical spectra for (c) Nyquist-SCM and (d) OFDM signals, and WDM spectra before and after the OBPF for (e) Nyquist-SCM and (f) OFDM signals with a $B_t$ of 14 GHz and a $\Delta v_{ch}$ of 19 GHz (non-overlapping case). Single channel optical spectra for (g) Nyquist-SCM and (h) OFDM signals, and WDM spectra after the OBPF for (i) Nyquist-SCM and (j) OFDM signals with a $B_t$ of 8.75 GHz and a $\Delta v_{ch}$ of 13 GHz (overlapping case). Note that frequency scales in optical spectra are relative to the optical carrier frequency of the central channel.

investigated in [19] and it was shown that a RRC filter roll-off factor of 0.3 with $f_{sc} = 0.75 f_s$ provides a good compromise between the ISD and receiver sensitivity. A transceiver design using these parameters was experimentally demonstrated to achieve WDM SSB Nyquist pulse-shaped single SCM QPSK transmission over standard SMF links of up to 800 km at a ISD of 1.3 b/s/Hz [19].

In this study, the performance of OFDM and single SCM formats with equivalent ISDs are compared; the symbol rate of the signals is kept constant at 7 GBaud, with gross bit-rates per channel of 14 and 28 Gb/s, respectively. The ISD is varied by varying the guard band ($B_g$) between the optical carrier and the sideband (hence changing the overlapping ratio parameter, $B_{ov}/B_s$), and the WDM channel spacing ($\Delta v_{ch}$). The performance of the signal formats is compared in terms of the required optical signal-to-noise ratio (OSNR) in back-to-back operation, and the maximum transmission distance over standard SMF links (including the effects of EDFA noise, fibre dispersion and nonlinearity). No digital or optical SSBI estimation/cancellation is carried out to avoid significant additional transceiver complexity in the system.

## III. Nyquist-SCM and OFDM System Models

The system diagrams for WDM Nyquist-SCM and OFDM signal generation, transmission and detection, that are modelled in MATLAB, are shown in Fig. 3(a) and Fig. 3(b) with the single channel and WDM optical spectra for the cases of channel bandwidths ($B_t$) of 14 and 8.75 GHz. Transmission simulations using the split-step Fourier method to solve the nonlinear Schrödinger equation (NLSE) were carried out for a range of values of $B_g$ and consequently, $B_t$ and $\Delta v_{ch}$. For the Nyquist-SCM simulations, a 7 GBaud conventional QPSK/16-QAM signal was generated using two/four de-correlated $2^{18}$ de Bruijn bit sequences. Subsequently, a pair of 256-tap RRC pulse shaping filter with a stop-band attenuation of 40 dB were applied to the in-phase (I) and quadrature (Q) components separately to achieve Nyquist QAM signalling as shown in Fig. 3(a). Then, Nyquist pulse-shaped signals were

up-converted to the subcarrier frequency and added to each other to obtain a double sideband Nyquist-SCM QAM signal. Following this, a sideband filter was applied digitally to obtain the SSB signal. In back-to-back operation, there was no need to apply clipping for the Nyquist-SCM signal since its PAPR value was equal to 8.0 dB which was sufficiently low. The PAPR of a complex signal is defined as

$$\text{PAPR} = \frac{\max[s(t)s^*(t)]}{E[s(t)s^*(t)]} \quad \text{and} \quad \text{PAPR}_{\text{dB}} = 10\log_{10}(\text{PAPR}) \quad (1)$$

where $s(t)$ is the complex signal, $t$ is the time index and $E[s(t)s^*(t)]$ is the expected value of the signal power. Note that PAPR value was found to be almost same for both QPSK and 16-QAM. Finally, digital electronic pre-distortion (EPD) [20], [21] and clipping [22] were applied to mitigate the chromatic dispersion accumulated at the targeted distance with a minimum penalty. The clipped signal can be formalized as

$$s_{\text{clipped}}(t) = \begin{cases} s(t) & \text{if} \quad |s(t)| \leq A \\ Ae^{jarg\{s(t)\}} & \text{if} \quad |s(t)| > A \end{cases} \quad (2)$$

where $s_{\text{clipped}}(t)$ represents the clipped signal, $A$ is the maximum amplitude value after clipping and $arg\{s(t)\}$ is the phase of $s(t)$, not affected by clipping. The clipping ratio (CR) is commonly defined as the ratio of the maximum to the average output power [23].

The OFDM signal generation is shown in Fig. 3(b). 128 data subcarriers were first modulated, and multiplexed using a 256-point inverse fast Fourier transform (IFFT). Then, a 2% cyclic prefix (CP) was added as a guard band to avoid the inter-symbol interference (ISI) due to filter delays introduced by electrical and optical filters in the system. Unlike Nyquist-SCM, clipping (1$^{\text{st}}$-stage) was applied to back-to-back OFDM signal (prior to EPD) to optimize its performance. Its PAPR was reduced from 14.8 dB to 11.3 dB. After clipping, similar to the Nyquist-SCM signal, EPD and clipping (2$^{\text{nd}}$-stage) were applied to the OFDM signal in the frequency domain to mitigate the dispersion with a minimum penalty (rather than using a longer CP) in order to operate at the same ISD as the Nyquist-SCM signal. The resolution of the DACs operating at 28 GSa/s was assumed to be 5 bits for both Nyquist-SCM and OFDM systems which was sufficient to avoid significant penalties ($\leq$ 0.5 dB) due to the quantization noise. It is expected that the use of high sampling rate DACs & ADCs will be acceptable in future low-cost systems, as the performance of silicon complementary metal oxide semiconductor (CMOS) technology continues to increase, and the cost & power consumption reduce. The electrical bandwidth of the transmitter and receiver were emulated using 5$^{\text{th}}$-order Bessel low-pass filters (LPFs) with an optimized bandwidth of $0.85f_s$. The optical carriers were added at the IQ-modulators being biased close to their quadrature points to achieve approximately linear mapping from the electrical to the optical domain with the desired optical carrier power. To model WDM transmission, all 7 WDM channels each carrying 28 Gb/s SSB Nyquist-SCM 16-QAM or the equivalent adaptively modulated OFDM signal were decorrelated by more than 170 ns (more than one symbol period).

The total bandwidth of a single channel ($B_t$) is the sum of $B_g$ and $B_s$ as shown in Fig. 2(a) and Fig. 3(c). To compare the ISD of modulation techniques fairly, $B_t$ was kept the same for both techniques. When the overlapping ratio was equal to 0, $B_s$ was set to 7 GHz at 7 GBaud, as can be seen in Fig. 3(c) and Fig. 3(d). In the case of non-zero overlapping ratio ($B_{ov} >$ 0 GHz so $B_t <$ 14 GHz), the SSBI decreases towards higher frequencies, so that the subcarriers close to the optical carrier are more significantly affected than those further away from the carrier. If the same constellation scheme is used for all subcarriers, the error probability is severely affected since it is dominated by the subcarriers with the highest distortion. To overcome this issue and, consequently, optimize the system performance, each subcarrier can be modulated with an optimally chosen format cardinality (also termed bit loading), so that similar bit error probabilities are experienced by all the subchannels. This bit loading can be adapted, according to the frequency dependent signal-to-noise ratio, and this technique is referred to as adaptively modulated OFDM. In the system considered in this paper, bit loading was applied depending on the signal-to-noise ratio (SNR) of each subcarrier using a "water-filling" approach with $M$-QAM modulation used for $M$ bits/symbol [24]. For the bit loading, the Levin-Campello (LC) algorithm was utilized since it provides an optimum discrete bit distribution (finite granularity) assuming the information granularity is the same for all subchannels which is usually the case [25]. The bits were allocated to the subcarriers by comparing the SNR threshold values for conventional modulation formats, *e.g.*, BPSK, QPSK *etc.*, and their received SNR values which were obtained from the receiver. Since their received SNR values also depend on the carrier-to-signal power ratio (CSPR), the optimum bit allocation was found by applying an exhaustive search for the CSPR value to achieve the best OSNR performance. For instance, to achieve a bit-rate of 28 Gb/s (requiring an average number of bits/symbol of 4 for the 7 GBaud signal), as the subcarriers overlapping with the signal-signal beating products had lower SNR values than the non-overlapping ones (see Fig. 4(a)), they were allocated lower numbers of bits per symbol (0, 1, 2 and 3 bits/sym). On the other hand, the subcarriers that did not overlap with the beating products were allocated with higher bits/symbol (4, 5 and 6 bits/sym) depending on their SNR values as shown in Fig. 4(b). The power was kept uniform across the subcarriers. The bit loading algorithm stopped when the desired bit-rate was achieved. Although bit loading significantly increases the receiver sensitivity compared to uniform modulation, it requires a feedback from the receiver to the transmitter to obtain the SNR values of each subcarrier [25], [26].

SNR, bit allocation and BER values per subcarrier at an OSNR of 26 dB, a CSPR of 13 dB and a $B_t$ of 8.75 GHz are shown in Fig. 4. At this $B_t$, 97 subcarriers (first subcarrier is the closest one to the optical carrier) overlapped with the signal-signal beating products. Since the distortion caused by the SSBI gradually decreased towards the higher frequencies due to the superposition of the subcarriers, each subcarrier was distorted by different amount of SSBI as shown in Fig. 4(a). The subcarriers that were distorted severely (57 subcarriers) were allocated with less than 4 bits per symbol. The ones

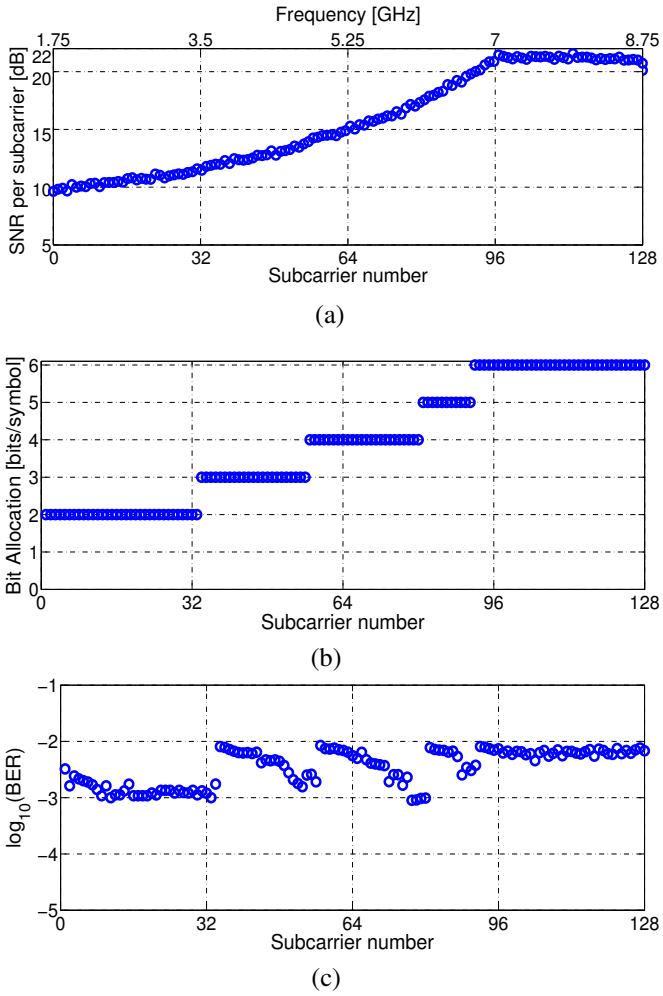


Fig. 4: OFDM bit loading for the case of a CSPR of 13 dB, an OSNR of 26 dB, and a $B_t$ of 8.75 GHz) at the HD-FEC limit. (a) SNR in dB per subcarrier, (b) bit allocation per subcarrier to achieve 28 Gb/s and (c) BER values per subcarrier.

that manage to maintain high SNR or do not even overlap with the beating products were allocated with the highest possible bits per symbol in order to achieve the desired bit-rate, that is 28 Gb/s. The BER for each subcarrier varied between $\sim 1\times10^{-3}$ and $8\times10^{-3}$. For the best receiver sensitivity performance, BER on each subcarrier should be the same. To equalize BER on each subcarrier, power loading in addition to the bit loading can be also applied instead of allocating the power equally across subcarriers. Nevertheless, at the same bit-rate, the system performance that utilizes power-and-bit loading is not significantly different than systems utilizing only bit loading [26]–[28]. For the case of the Nyquist-SCM system, $\alpha$ was varied from 0 to 0.3 and $f_{sc}$ was adjusted accordingly whilst ensuring that Nyquist-SCM and OFDM signals had equal $B_t$ values as shown in Fig. 3(e) and Fig. 3(f). Table I shows the optical bandwidth (BW) and ISD values considered in the simulations. In both cases, $\Delta v_{ch}$ was chosen such that there was negligible linear crosstalk penalty between the channels and net ISD is calculated assuming 16-QAM and a 7% HD-FEC overhead.

The transmission link considered in the simulations was uncompensated standard SMF and the fibre parameters

TABLE I: Optical BW and ISD values used in the simulations

| $B_t$ (GHz) | $B_s$ (GHz) | $B_g$ (GHz) | $B_{ov}$ (GHz) | $\Delta v_{ch}(GHz)$ | Net ISD (b/s/Hz) |
|---|---|---|---|---|---|
| 14 | 7 | 7 | 0 | 19 | 1.37 |
| 8.75 | 7 | 1.75 | 5.25 | 13 | 2.0 |

$\alpha, D, \gamma$, Erbium-doped fibre amplifier (EDFA) noise figure and span length were chosen as 0.2 dB/km, 16.8 ps/(nm.km), 1.2 $W^{-1}km^{-1}$, 5 dB and 80 km, respectively. The EDFA was set to compensate the fibre loss over each span which had 16 dB attenuation. All amplified spontaneous emission (ASE) noise generated by the EDFAs was added inline to model nonlinear signal-ASE interaction. The single channel and WDM signal transmission in the fibre was modelled using the symmetrical split-step Fourier method [29] with step sizes of 1 km and 0.4 km, respectively at a bandwidth of ~200 GHz.

A 3rd-order super-Gaussian OBPF with a bandwidth of 17 GHz ($\Delta v_{ch}=19$ GHz) and 11 GHz ($\Delta v_{ch}=13$ GHz) was utilized to demultiplex the central WDM channel for $B_t=14$ and 8.75 GHz, respectively. Then, the filtered channel was detected by a single-ended photodiode with a responsitivity of 1 A/W. The resolution and sampling rate of the ADC were assumed to be 5-bit and 28 GSa/s, respectively. The DACs/ADC resolution and the bandwidth of the Bessel LPFs for both modulation formats were chosen such that the implementation penalty was kept within 1 dB for both single channel and WDM transmission. After the detection and digitization, the Nyquist-SCM signal was first down-converted to baseband and consequently, a matched RRC filter ($\alpha=0.3$) was applied. For optimum sampling, a 5-tap equalizer using least mean squares (LMS) adaptation was applied as shown in Fig. 3(a). The equalizer first utilized the constant modulus algorithm (CMA) as a cost function to update the filter taps for fast convergence and then, switched to decision directed LMS.

In the OFDM case, the digitized detected signal was first converted from serial to parallel and consequently, the CP was removed from the received signal. Note that no symbol/frame timing synchronization algorithm was applied in our OFDM simulation model for simplicity since the sampling rate of DACs and ADC are the same. Following this, a 256-point FFT was applied and the channel estimation was performed using a single-tap equalizer to cancel the phase errors and distortions incurred along the transmission path as shown in Fig. 3(b). Training symbols have the same data sequence compared to the data used. They were inserted periodically, every 63 data symbols leading to a 1% overhead, a technique also referred to as block-type channel estimation. The estimation was based on a least-square method so that the coefficients of the single-tap equalizer were derived by comparing the received training symbols with the transmitted ones [30]. To improve the channel estimation performance, a polynomial fit was applied to the derived coefficients. Finally, the received signal was multiplied with the inverse of the estimated channel response to restore the transmitted signal. After equalization, the symbol-to-bit demapping was performed and BER was calculated by counting the errors using $2^{18}$ bits in both setups. The simulation results are discussed in Section IV.

## IV. Results and Discussions

### A. Back-to-back

First, back-to-back single channel Nyquist-SCM QPSK/16-QAM and the equivalent adaptively modulated OFDM signals were simulated to determine the receiver sensitivities as shown in Fig. 5(a)/Fig. 5(b). Then, at the HD-FEC limit assuming 7% overhead, the signals were compared at different values of signal bandwidth ($B_t$), presented in Fig. 6. Note that, $\alpha$ was set to 0 when $B_{ov}$ was set 0. However, with $B_t$ set to less than 14 GHz, $\alpha$ for the Nyquist-SCM signal was relaxed from 0 to 0.3 to achieve a better OSNR performance through increasing its tolerance to SSBI due to averaging the distortion across the signal bandwidth and reducing its PAPR whilst adjusting the RF subcarrier frequency to keep $B_t$ and the ISDs identical to those of the OFDM signal. When Nyquist-SCM QPSK is used at a $B_t$ of 14 GHz, the required OSNR for Nyquist-SCM is very similar to (approximately 0.5 dB lower than) the equivalent OFDM signal. This performance difference is due to the higher PAPR value of the OFDM signal. With the PAPR of the OFDM signal optimized (by clipping and minimizing the required OSNR) for a 5-bit DAC resolution, its value is still 3.3 dB higher than the PAPR of the Nyquist-SCM signal, calculated using Eq. 1. This difference leads to a higher required optical carrier power to avoid any clipping upon photodetection for the OFDM signal, and hence the higher required OSNR.

It was found that the performance difference between Nyquist-SCM and OFDM signals at $B_t \geq 8.75$ GHz did not differ significantly until the highest ISD was reached. However, when $B_t$ was less than 8.75 GHz, the required OSNR values for the two signal formats diverged significantly. The Nyquist-SCM format required an OSNR of 12.0 dB at $B_t =$ 7 GHz, while the corresponding value for the OFDM signal was found to be 16.1 dB, 4 dB higher than Nyquist-SCM (see Fig. 6). When the Nyquist-SCM modulation format was switched from QPSK to 16-QAM (and the bit distribution on the OFDM subcarriers also increased to achieve equivalent ISD values), they had similar OSNR requirements for $B_t \geq$ 10.5 GHz. However, at $B_t = 8.75$ GHz, the required OSNR difference between Nyquist-SCM and OFDM signals became again approximately 4 dB. With $B_t$ set to 7 GHz, at which point the gross ISD, 4 b/s/Hz, is close to $\log_2(M)$, neither system was able to achieve the HD-FEC limit BER of $3.8 \times 10^{-3}$.

The performance difference between the two formats can be explained by two reasons: 1) Nyquist SCM signal averages the distortion due to the signal-signal beating interference in the entire signal bandwidth whereas the subcarriers in OFDM signal overlapping with the beating interference are severely affected even though they are modulated adaptively. 2) Nyquist-SCM signal has lower PAPR than the OFDM signal which reduces the required optical carrier power, and consequently, the required OSNR for optimum detection. It is worth noting that the slope of the BER versus OSNR curves in Fig. 5(a)/Fig. 5(b) changes when $B_t$ is less than 8.75/10.5 GHz due to the signal-signal beating interference.

In DD systems, optimizing the CSPR is essential to achieve a trade-off between signal-ASE beating noise and SSBI. When

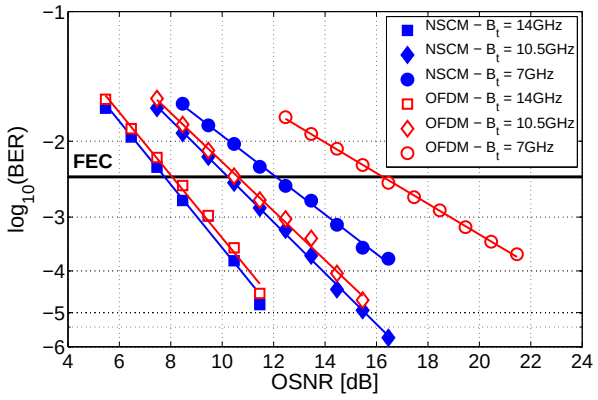


(a)

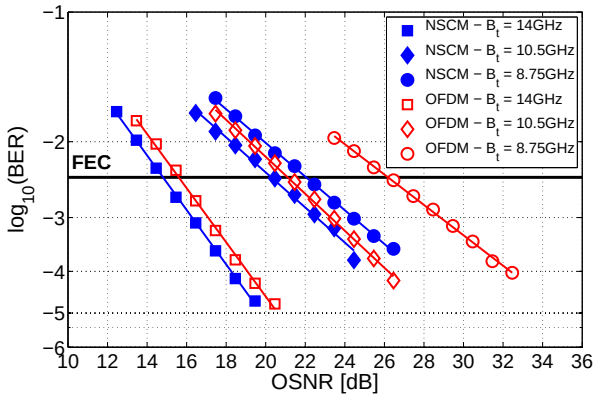


(b)

Fig. 5: Back-to-back BER with respect to OSNR with different values of signal bandwidth ($B_t$) for (a) Nyquist-SCM QPSK and the equivalent adaptively modulated OFDM signals at 14 Gb/s and (b) Nyquist-SCM 16-QAM and the equivalent adaptively modulated OFDM signals at 28 Gb/s.

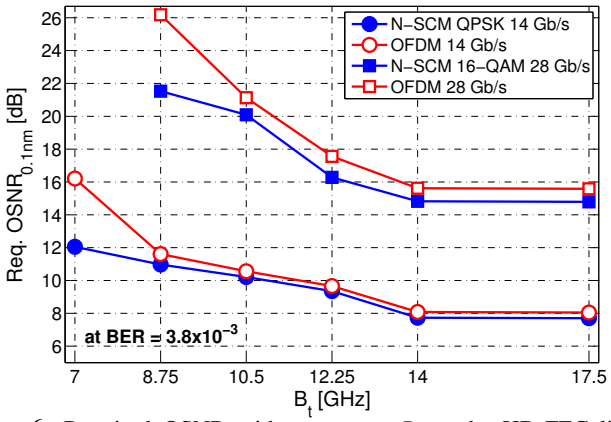


Fig. 6: Required OSNR with respect to $B_t$ at the HD-FEC limit for Nyquist-SCM QPSK/16-QAM and the equivalent adaptively modulated OFDM signals.

$B_t = 14$ GHz, at the OSNR values giving a BER of $3.8 \times 10^{-3}$, the optimum CSPR values for both QPSK and 16-QAM were found to be -5 dB and 0 dB for Nyquist-SCM and OFDM signal formats, respectively. The difference in CSPR values is explained by the difference in PAPR of the signals after clipping. On the other hand, in the case where the signal overlaps with the SSB products (*i.e.*, $B_t < 14$ GHz), the carrier-

signal beating products have to be large enough compared to the SSBI to be recovered. Thus, the optimum CSPR value increases with reducing $B_t$. At $B_t = 8.75$ GHz, the optimum CSPR value in the case of 16-QAM was found to increase to 6 and 13 dB for the Nyquist-SCM and OFDM signals, respectively, at the HD-FEC limit. This increase in CSPR directly translates into the penalties in the required OSNR as seen in Fig. 5 and Fig. 6. Better performance of Nyquist-SCM at high ISD was also observed in [31]. Single channel vestigial sideband Nyquist-SCM was compared with OFDM in back-to-back and transmission performance over 100 km, although without considering any adaptive bit loading for the OFDM signal or EPD to mitigate the chromatic dispersion.

### B. Transmission Results

Following the back-to-back simulations described above, both single channel and 7-channel WDM transmission simulations at 28 Gb/s per channel were carried out. In each case, the WDM channel spacing ($\Delta v_{ch}$) was chosen such that a negligible penalty ($\leq$ 0.5 dB) resulted due to linear inter-channel crosstalk. Initially, the signal bandwidth $B_t$ was set to 14 GHz ($B_s = B_g = 7$ GHz so that $B_{ov} = 0$ GHz) and a $\Delta v_{ch}$ of 19 GHz was chosen (resulting in a net ISD of 1.37 b/s/Hz assuming 7% HD-FEC overhead). Fig. 7(a) shows the range of launch powers at which the pre-FEC BER was $< 3.8 \times 10^{-3}$. Due to the low crosstalk between channels, the transmission performance of single channel and WDM are very similar in the linear regime. However, in the non-linear regime in single channel transmission, the lower maximum launch powers indicate that OFDM is more sensitive to self-phase modulation (SPM) than Nyquist-SCM. Nyquist-SCM has 2 dB greater margin compared to the OFDM signal. This margin was reduced to 0.8 dB in WDM transmission. At $B_{ov} = 0$ GHz or $B_t = 14$ GHz, the maximum transmission distance of Nyquist-SCM and OFDM signals were quite similar, (1880 km vs 1720 km, respectively) which was expected from the result, shown in Fig. 6.

Next, $B_t$ was reduced from 14 to 8.75 GHz and consequently, it was possible to reduce $\Delta v_{ch}$ from 19 to 13 GHz, resulting in an increase in the net ISD from 1.37 to 2.0 b/s/Hz. The single channel and the WDM transmission results at this ISD are presented in Fig. 7(b). In both single channel and WDM transmission cases, Nyquist-SCM offered a maximum transmission distance approximately two times larger than the OFDM signal. This difference is mainly due to ~4 dB difference in the required OSNR observed in back-to-back operation between the Nyquist-SCM and the OFDM formats as shown in Fig. 5(b) and Fig. 6. Accordingly, the WDM Nyquist-SCM signal could be transmitted over distances of up to 720 km of standard SMF whereas the maximum distance with WDM OFDM was just 320 km. The maximum transmission distances of single channel and WDM system for the Nyquist-SCM 16-QAM and the equivalent adaptively modulated OFDM signals are summarized in Fig. 8.

Further studies are required comparing the performance of Nyquist-SCM with other spectrally-efficient modulation techniques, such as asymmetrically clipped optical OFDM [32], and carrierless amplitude phase (CAP) modulation [3], [33].

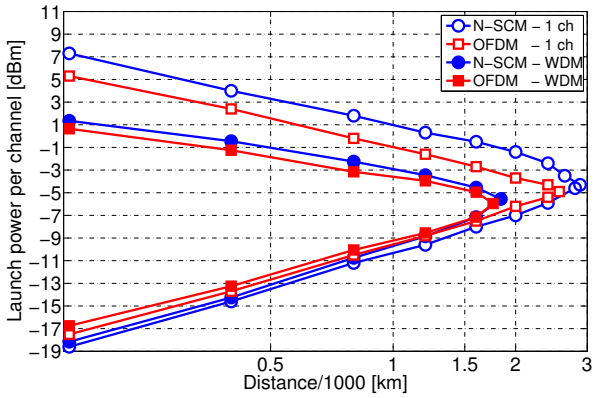


(a)

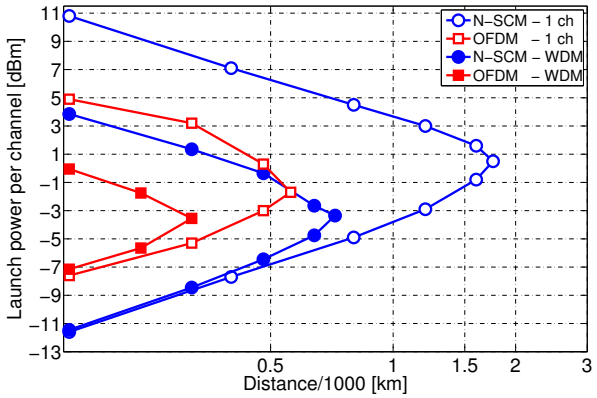


(b)

Fig. 7: At BER$= 3.8 \times 10^{-3}$, single channel and WDM transmission performance of 28 Gb/s Nyquist-SCM 16-QAM and the equivalent adaptively modulated OFDM signals at net ISD of (a) 1.37 b/s/Hz ($B_t = 14$ GHz and $\Delta v_{ch} = 19$ GHz) and (b) 2.0 b/s/Hz ($B_t = 8.75$ GHz and $\Delta v_{ch} = 13$ GHz.

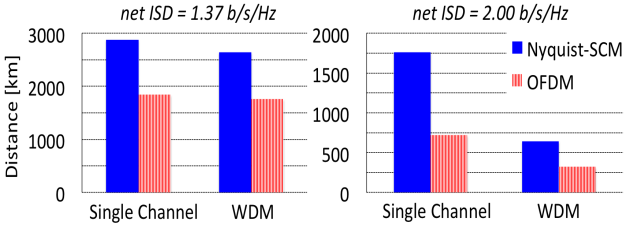


Fig. 8: Maximum transmission distances of single channel and WDM systems for 28 Gb/s Nyquist-SCM and OFDM signals at net ISD of 1.37 b/s/Hz (left) and (b) 2 b/s/Hz (right).

Additionally, the use of DSP-based SSBI mitigation methods, which can provide further performance improvements, needs detailed investigation [8], [13].

## V. Summary and Conclusions

We compared two direct-detection modulation formats, Nyquist-SCM and OFDM. Both techniques can be used to achieve high ISD (>1 b/s/Hz) transmission. The aim of the comparison in this paper was to assess their tolerance to signal-signal beating interference at high ISDs as the spectral guard band between the optical carrier and sideband was varied. The roll-off factor of the pulse shaping filter and RF-subcarrier frequency were optimised for the Nyquist-SCM signal whereas bit loading was carried out with the OFDM signal to optimise their tolerance to the SSBI. The performance comparison using QPSK and 16-QAM signalling operating at 7 GBaud per

channel for the back-to-back case showed similar required OSNR values for Nyquist-SCM and OFDM signal formats, at the HD-FEC limit of $3.8 \times 10^{-3}$ when a large spectral guard band ($B_g \geq 7$ GHz, $B_t \geq 14$ GHz) between the optical carrier and sideband was used. However, the Nyquist-SCM QPSK/16-QAM signal outperformed the equivalent adaptively modulated OFDM signal when the spectral guard band was lower than 8.75/10.5 GHz, leading to ∼75%/50% overlap between the signal-signal beating products and sideband, respectively. This can be explained by the averaging of the nonlinear distortion caused by the beating interference over the entire signal bandwidth and the lower PAPR of the Nyquist-SCM signal. Following the assessment of back-to-back performance, single channel and WDM transmission performance of the Nyquist-SCM and OFDM signals were compared by simulations at net ISDs of 1.37 b/s/Hz ($B_t = 14$ GHz) and 2.0 b/s/Hz ($B_t$=8.75 GHz). The results showed that the single channel and WDM system performance of both signal formats were very similar at the lower ISD. However, at 2.0 b/s/Hz, their performance diverged. 7-channel WDM Nyquist-SCM and the OFDM signals can be transmitted over standard SMF distances of up to 720 and 320 km, respectively. Direct detection Nyquist-SCM appears to have a higher tolerance to the SSBI and has the potential to offer the combination of higher ISD, and/or longer transmission distances with low complexity transceiver design for metro, regional, access and back-haul applications.

## ACKNOWLEDGMENTS

The authors would like to thank Dr. Colm Browning from the Radio and Optical Communications Lab at Dublin City University for his stimulating discussion.

## REFERENCES

[1] P. Winzer, "High spectral-efficiency optical modulation formats," *J. Lightw. Technol.*, vol. 30, no. 24, pp. 3824–3835, 2012.

[2] A.H. Gnauck *et al.*, "High-capacity optical transmission systems," *J. Lightw. Technol.*, vol. 26, no. 9, pp. 1032–1045, 2008.

[3] J.L. Wei *et al.*, "Performance and power dissipation comparisons between 28 Gb/s NRZ, PAM, CAP and optical OFDM systems for data communication applications," *J. Lightw. Technol.*, vol. 30, no. 20, pp. 3273–3280, 2012.

[4] E. Pincemin *et al.*, "Experimental performance comparison of duobinary and PSBT modulation formats for long-haul 40 Gb/s transmission on G 0.652 fibre," *Opt. Express*, vol. 20, no. 27, pp. 28171–28190, 2012.

[5] M. Alfiad and S. Tibuleac, "100G superchannel transmission using 4×28 Gb/s subcarriers on a 25-GHz Grid," *IEEE Photon. Technol. Lett.*, vol. 27, no. 2, pp. 157–160, 2015.

[6] M. Schuster *et al.*, "Spectrally efficient compatible single-sideband modulation for OFDM transmission with direct detection," *IEEE Photon. Technol. Lett.*, vol. 20, no. 9, pp. 670–6728, 2008.

[7] Y. Zhang *et al.*, "Theoretical and experimental investigation of compatible SSB modulation for single channel long-distance optical OFDM transmission," *Opt. Express*, vol. 18, no. 16, pp. 16751–16764, 2010.

[8] Z. Cao *et al.*, "Direct-detection optical OFDM transmission system without frequency guard band," *IEEE Photon. Technol. Lett.*, vol. 22, no. 11, pp. 736–738, 2010.

[9] W.R. Peng *et al.*, "Spectrally efficient direct-detected OFDM transmission employing an iterative estimation and cancellation technique," *Opt. Express*, vol. 17, no. 11, pp. 9099–9111, 2009.

[10] S.A. Nezamalhosseini *et al.*, "Theoretical and experimental investigation of direct detection optical OFDM transmission using beat interference cancellation receiver," *Opt. Express*, vol. 21, no. 13, pp. 15237–15246, 2013.

[11] J. Ma, "Simple signal-to-signal beat interference cancellation receiver based on balanced detection for a single-sideband optical OFDM signal with a reduced guard band," *Opt. Lett.*, vol. 38, no. 21, pp. 4335–4338, 2013.

[12] A.J. Lowery, "Amplified-spontaneous noise limit of optical OFDM lightwave systems," *Opt. Express*, vol. 16, no. 2, pp. 860-865, 2008.

[13] W.R. Peng *et al.*, "Spectrally efficient direct-detected OFDM transmission incorporating a tunable frequency gap and an iterative detection techniques," *J. Lightw. Technol.*, vol. 27, no. 24, pp. 5723–5735, 2009.

[14] A.J. Lowery and L.B. Du, "Optical orthogonal division multiplexing for long haul optical communications: A review of the first five years," *Opt. Fiber Technol.*, vol. 17, pp. 421–438, 2011, Invited paper.

[15] J. Armstrong, "OFDM for optical communications," *J. Lightw. Technol.*, vol. 27, no. 3, pp. 189–204, 2009.

[16] A.O.J. Wiberg *et al.*, "Single cycle subcarrier modulation," in *Proc. Opt. Fiber Commun. (OFC) Conf.*, Mar. 2009, paper OTuE.1.

[17] A.S. Karar and J.C. Cartledge, "Generation and detection of a 56 Gb/s signal using a DML and half-cycle 16-QAM Nyquist-SCM," *IEEE Photon. Technol. Lett.*, vol. 25, no. 8, pp. 757–760, 2013.

[18] G. Bosco *et al.*, "Performance limits of Nyquist-WDM and CO-OFDM in high-Speed PM-QPSK systems," *IEEE Photon. Technol. Lett.*, vol. 22, no. 15, pp. 1129–1131, 2010.

[19] M.S. Erkılınç *et al.*, "Nyquist-shaped dispersion-precompensated subcarrier modulation with direct detection for spectrally-efficient WDM transmission," *Opt. Express*, vol. 22, no. 8, pp. 9420–9431, 2014.

[20] R.I. Killey *et al.*, "Electronic dispersion compensation by signal predistortion using digital processing and a dual-drive Mach–Zehnder modulator," *IEEE Photon. Technol. Lett.*, vol.17, no.3, pp.714–716, 2005.

[21] M.S. Erkilinc *et al.*, "Nyquist-shaped dispersion-precompensated subcarrier modulation with direct detection," *Proc. OFC Conf.*, Mar. 2014, paper Th3K.4.

[22] M.S. Erkılınç *et al.*, "Effect of clipping on the performance of Nyquist-shaped dispersion-precompensated subcarrier modulation transmission with direct detection," *Proc. European Conf. on Opt. Commun.*, Sep. 2014, paper Tu.3.3.1.

[23] C.R. Berger *et al.*, "Theoretical and experimental evaluation of clipping and quantization noise for optical OFDM," *Opt. Express*, vol. 19, no. 18, pp. 17713–17728, 2011.

[24] R.P. Giddings *et al.*, "Experimental demonstration of a record high 11.25 Gb/s real-time optical OFDM transceiver supporting 25km SMF end-to-end transmission in simple IMDD systems, " *Opt. Express*, vol. 18, no. 6, pp. 5541–5555, 2010.

[25] J.M. Cioffi, "Course notes", Ch.4, pp. 317-323, [Online]. Available: http://www.stanford.edu/group/cioffi/book.

[26] D. Bykhovsky and S. Arnon, "An experimental comparison of different bit-and-power allocation algorithms for DCO-OFDM," *J. Lightw. Technol.*, vol. 32, no. 8, pp. 1559–1564, 2014.

[27] X.Q. Jin *et al.*, "Experimental demonstrations and extensive comparisons of end-to-end real-time optical OFDM transceivers with adaptive bit and/or power loading," *IEEE Photon. J.*, vol. 3, no. 3, pp. 500–511, 2011.

[28] E. Giacoumidis *et al.*, "Adaptive loading algorithms for IMDD optical OFDM PON systems using directly modulated lasers," *J. Opt. Commun. and Network.*, vol. 4, no. 10, pp. 769–778, 2012.

[29] G.P. Agrawal, "Applications of nonlinear fiber optics", 3rd ed., *Academic press*, 2010.

[30] J.-J. van de Beek *et al.*, "On channel estimation in OFDM systems," *Proc. IEEE Veh. Technol. Conf.*, Jul. 1995, vol. 2, pp. 815-819.

[31] N. Liu *et al.*, "40-Gbps vestigial sideband half-cycle Nyquist subcarrier modulation transmission experiment and its comparison with orthogonal frequency division multiplexing," *Opt. Eng.*, vol. 53, no. 9, pp. 096114–096114, 2014.

[32] S.D. Dissanayake and J. Armstrong, "Comparison of ACO-OFDM, DCO-OFDM and ADO-OFDM in IM/DD systems," *J. Lightw. Technol.*, vol. 31, no. 7, pp. 1063–1072, 2013.

[33] J.L. Wei *et al.*, "Study of 100 gigabit ethernet using carrierless amplitude/phase modulation and optical OFDM," *J. Lightw. Technol.*, vol. 31, no. 9, pp. 1367–1373, 2013.